DOI: 10.1002/ejic.201000671

$Li_2CaSi_2N_4$ and $Li_2SrSi_2N_4$ – a Synthetic Approach to Three-Dimensional Lithium Nitridosilicates

Martin Zeuner,[a] Sandro Pagano,[a] Stephan Hug,[a] Philipp Pust,[a] Sebastian Schmiechen,[a] Christina Scheu,[a] and Wolfgang Schnick*[a]

Keywords: Solid-state reactions / Lithium / Nitridosilicates / Solid-state NMR

The quaternary lithium alkaline earth nitridosilicates $Li_2MSi_2N_4$ with M = Ca, Sr were synthesized at 900 °C by employment of liquid lithium as fluxing agent in weld shut tantalum ampoules. The title compounds crystallize in space group $Pa\bar{3}$ [$Li_2CaSi_2N_4$: a = 1056.9(12) pm, Z = 12, R_1 = 0.0439, $wR2$ = 0.0839, 412 data, 42 parameters; $Li_2SrSi_2N_4$: a = 1071.37(12) pm, Z = 12, R_1 = 0.0476, $wR2$ = 0.1227, 528 data, 42 parameters]. The structure is built up from vertex sharing [SiN_4] tetrahedra forming a three-dimensional network comprising the alkaline earth and lithium ions in the voids. The network is the first example of a nitridosilicate adopting topology of *Net 39* according to O'Keeffe. The two crystallographically independent M^{2+} sites are highly symmetrically coordinated by six nitrogen atoms. Lattice energy calculations (MAPLE) and EDX measurements confirmed the electrostatic bonding interactions and the chemical compositions. ^{7}Li and ^{29}Si solid-state MAS NMR spectra of $Li_2SrSi_2N_4$ are reported. Electron energy-loss spectroscopy (EELS) elucidates further information upon the lithium incorporation.

Introduction

During the last few years, research on nitridosilicates and related compounds (e.g. SiONS and SiAlONs) has been an emerging and rapidly growing field in materials chemistry. These compounds found broad application as functional or structural materials, e.g. due to their exceptional chemical and physical stability in conjunction with nonlinear optical properties (second harmonic generation, SHG) or as highly efficient phosphors in modern LED technology upon doping with Ce^{3+} or Eu^{2+}.[1–6] The wide diversity of condensed silicate structures is a direct consequence of the variability in connectivity of oxygen in classical silicates and even more of nitrogen in nitridosilicates.[7] Whereas the structural chemistry of oxosilicates is limited to terminal $O^{[1]}$ atoms and simply bridging $O^{[2]}$, nitridosilicates emulate the same with $N^{[1]}$ atoms and $N^{[2]}$ but can additionally form highly crosslinked networks which contain $N^{[3]}$ or even $N^{[4]}$ bridges connecting up to four neighboring tetrahedral centers (cf. $BaYbSi_4N_7$).[8,9] Commonly, nitridosilicates (e.g., $M_2Si_5N_8$ with M = Ca, Sr, Eu or Ba) have been synthesized at high temperatures around 1400–1600 °C starting from the respective metals or oxides and silicon nitride or silicon diimide [$Si(NH)_2$], leading predominantly to three-dimensional framework silicates.[7,10,11] Recently, we have reported on a low temperature approach to synthesize nitridosilicates involving supercritical ammonia and metal amides.[12,13] In contrast, the use of alkali metal melts (e.g. sodium) yielded $Ba_5Si_2N_6$, the first group-like nitridosilicate consisting of edge-sharing $[Si_2N_6]^{10-}$ units.[14] The low synthesis temperature of 760 °C seems to afford structures with low degree of condensation. By employment of liquid sodium as a fluxing agent and decomposition of sodium azide as nitrogen source nitridosilicates $MSiN_2$ (M = Ca, Sr, Ba) have become available as well.[15] Recently, we reported on a modified flux approach utilizing liquid lithium for the synthesis of nitridosilicates. The reactions were conducted in closed tantalum ampoules at relatively low temperatures of 900 °C. Systematic investigations led to the discovery of novel compounds covering the whole range of dimensionality of [SiN_4] building blocks from group-type ions ($Li_4Ca_3Si_2N_6$) through chains ($LiCa_3Si_2N_5$, Eu_2SiN_3, $Li_5Ln_5Si_4N_{12}$ with Ln = La, Ce)[16,17] up to frameworks ($Li_2Sr_4Si_4N_8O$).[18] We assume that the nitrogen pressure inside the ampoule is a crucial parameter for the condensation of [SiN_4] tetrahedra. The nitrogen content is controlled by the use of Li_3N or LiN_3. Since a number of less condensed nitridosilicates became now accessible, we focused in this contribution on the synthesis of air-stable framework silicates, obtainable at low reaction temperatures by the employment of the lithium flux method. In this context, we investigated the influence of N_2 upon the synthesis of lithium nitridosilicates.

Here, we present two new quaternary lithium alkaline earth nitridosilicates, namely $Li_2MSi_2N_4$ (M = Ca, Sr), comprising a three-dimensional network unprecedented for silicates so far. The material is air-stable and not moisture

[a] Ludwig-Maximilians-Universität München,
Department Chemie
Butenandtstraße 5–13 (D), 81377 München, Germany
Fax: +49-89-2180-77440
E-mail: wolfgang.schnick@uni-muenchen.de

Supporting information for this article is available on the WWW under http://dx.doi.org/10.1002/ejic.201000671.

sensitive and was characterrized by X-ray diffraction, ^{7}Li and ^{29}Si solid-state MAS NMR spectra, scanning electron microscopy (SEM), transmission electron microscopy (TEM), and electron energy-loss spectroscopy (EELS) measurements performed in the TEM.

Results and Discussion

Influence of Nitrogen Pressure

As already mentioned, a number of nitrides have been synthesized in liquid sodium employing decomposition of NaN_3 as a nitrogen source.[15] Analogously, we conducted the reaction of alkaline earth metals and silicon diimide [$Si(NH)_2$] with LiN_3 in molten lithium. The reactions were performed in weld-shut tantalum ampoules. Albeit the decomposition of LiN_3 in the presence of lithium metal yields Li_3N, we obtained completely different products when starting from LiN_3 instead of Li_3N. We observed the predominant development of less condensed Si/N substructures by use of Li_3N. The use of Li_3N in the appropriate atomic ratio with lithium led to group-type ($Li_4Ca_3Si_2N_6$) and chain-type ($LiCa_3Si_2N_5$) nitridosilicates, respectively, whereas LiN_3 and Li_2O favored the formation of $Li_2O@[SrSiN_2]_4$ (cf. Scheme 1).[18]

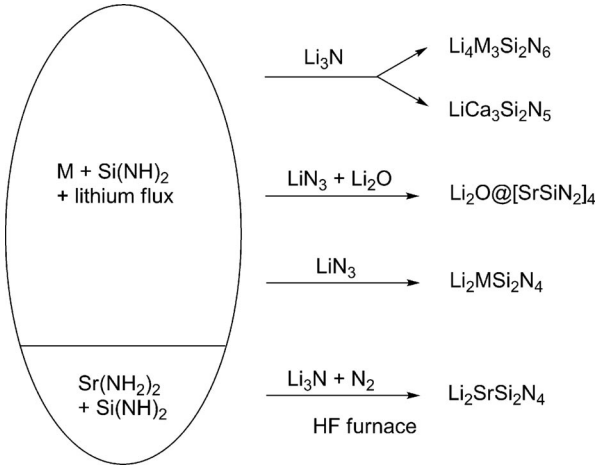

Scheme 1. Influence of the nitrogen content of the starting materials upon the formation of different lithium nitridosilicates at 900 °C (M = Ca, Sr).[18]

The syntheses of $Li_2MSi_2N_4$ (M = Ca, Sr) were performed in weld shut tantalum ampoules by reaction of the respective alkaline earth metals with $Si(NH)_2$, LiN_3 and lithium. The combination of LiN_3 and oxygen free starting materials led to these highly condensed nitridosilicates. Presumably, the specific amount of nitrogen in the reaction mixture plays an important role since decomposition of LiN_3 significantly raises the nitrogen pressure inside the ampoules and nitridosilicates with a higher degree of condensation are obtained. However, the pressure inside the tantalum ampoules can only be estimated since this setup allows no exact pressure determination. In the case of $Li_2SrSi_2N_4$, we developed a second synthetic approach using reactive strontium amide, silicon diimide and Li_3N as starting materials in an open system by using tungsten crucibles in high-frequency furnaces.[19] The formation of $Li_2CaSi_2N_4$ seems to require a slightly higher nitrogen pressure which cannot be realized by the high-frequency approach. We conclude that the synthesis of $Li_2MSi_2N_4$ is solely successful under nitrogen atmosphere (Scheme 1).

However, synthesis of $Li_2MSi_2N_4$ with M = Ca, Sr in tantalum ampoules yielded significantly larger single crystals compared to the synthesis under nitrogen. The spheroid like shaped crystals already suggested a highly symmetrical crystal system (cf. Figure 1). Phase-pure bulk samples of $Li_2SrSi_2N_4$ for solid-state NMR and EELS measurements were synthesized via the HF furnace route in order to obtain a homogeneous product with no residuals of elemental lithium. As the compounds are resistant to oxygen and water, the colorless crystals can be isolated from side products by washing with EtOH. A powder X-ray diffraction pattern of $Li_2SrSi_2N_4$ compared with patterns calculated from single-crystal data can be found in the Supporting Information (Figure S1).

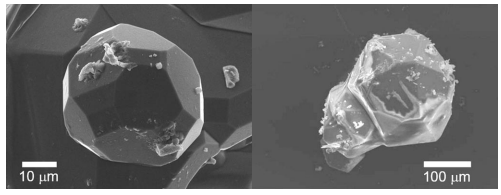

Figure 1. SEM images of $Li_2CaSi_2N_4$ (left) and $Li_2SrSi_2N_4$ (right).

Crystal Structure of $Li_2MSi_2N_4$ with M = Ca, Sr

$Li_2MSi_2N_4$ with M = Ca, Sr crystallizes in the cubic space group $Pa\bar{3}$ and comprises a three-dimensional nitridosilicate network with exclusively corner-sharing [SiN_4] tetrahedra. Details of the single-crystal X-ray diffraction analysis, atomic coordinates, and equivalent displacement parameters are listed in Tables 1, 2, and 4. The crystal structure is in detail described for $Li_2CaSi_2N_4$, however all the corresponding crystallographic information for $Li_2SrSi_2N_4$ can be found in the Supporting Information (Tables S1 and S2). The N atoms are bound covalently to two Si atoms (Figure 2), in contrast to nitridosilicates with single-bonded ($Li_4Ca_3Si_2N_6$)[18] or triple-bonded N atoms ($Ca_2Si_5N_8$).[20]

Table 1. Atomic coordinates and equivalent displacement parameters for $Li_2CaSi_2N_4$.

Atom		*x*	*y*	*z*	U_{eq}[a]
Ca1	8*c*	0.20499(5)	0.20499(5)	0.20499(5)	0.0103(3)
Ca2	4*b*	1/2	0	0	0.0169(3)
Si1	24*d*	0.48475(7)	0.37258(7)	0.25162(7)	0.0073(2)
N1	24*d*	0.2813(2)	0.1097(2)	0.0036(2)	0.0096(5)
N2	24*d*	0.2759(2)	0.1378(2)	0.4214(2)	0.0128(5)
Li1	24*d*	0.2217(6)	–0.0476(5)	0.1136(5)	0.0207(11)

[a] U_{eq} is defined as 1/3 of the trace of the U_{ij} tensors.

The compounds exhibit a degree of condensation $\kappa = 0.5$ identical with that of SiO_2 or $MSiN_2$ (M = Be, Mg, Ca, Sr, Ba, Mn, Zn).[15,21–23]

Table 2. Selected interatomic distances /pm for $Li_2CaSi_2N_4$.

Ca1–N1	248.9(2)	3×	Si1–N2	171.4(3)
Ca1–N2	251.0(3)	3×	Si1–N2	172.2(3)
Ca2–N1	258.6(2)	6×	Li1–N1	212.4(6)
Ca1–Li1	284.4(5)	3×	Li1–N1	219.9(6)
Ca1–Li1	289.3(5)	3×	Li1–N2	224.4(6)
Si1–N1	173.6(2)		Li1–N2	229.2(6)
Si1–N1	176.6(2)		Li1–N2	241.5(6)
			Ca1–Ca2	437.1(6)

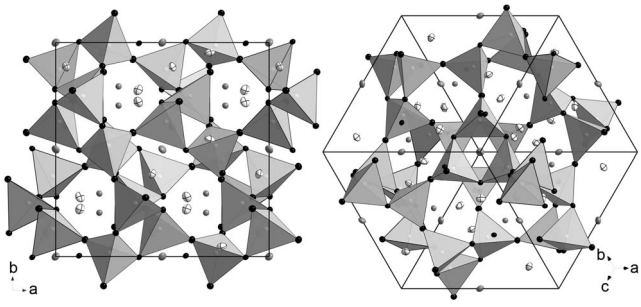

Figure 2. Unit cell of $Li_2CaSi_2N_4$: view along [001] (left); view along [111] (right), two *dreier* rings can be observed along the threefold axis; Ca atoms gray, [SiN_4] units are depicted as closed gray polyhedrons, N atoms black and Li ions white with black stripes (ellipsoids with a probability of 50%).

The [SiN_4] tetrahedra framework is built up from *dreier* rings forming *siebener* rings (Figure 3).[24] This network is the first nitridosilicate representative of *Net39* according to the classification of cubic unit cells from O'Keeffe regarding unit cells consisting of 24 tetrahedra (8 *dreier* rings, 6 *siebener* rings).[25] The *dreier* rings are perpendicular to the four threefold axes, respectively. Furthermore, *Net*39 is unprecedented for silicates so far. This might be due to *dreier* rings being unfavored and less frequent in condensed oxosilicates. The structure of $Li_2MSi_2N_4$ (M = Ca, Sr) is closely related to the high-pressure modifications of the borates MB_2O_4 (M = Ca, Sr), which are reported to crystallize in *Net39*.[26,27] Moreover, this structural motif can also be observed in ternary sulfides such as $BaGa_2S_4$ and $BaAl_2S_4$.[28] The distances Si–N in $Li_2CaSi_2N_4$ range between 171.4(4) and 176.6(2) pm and are typical for nitridosilicates (Table 2).[7] The N1 atoms exclusively connect the tetrahedra of the *dreier* rings, whereas each *dreier* ring unit participates with two N2 atoms to one *siebener* ring, which is connected through three N1 and four N2 atoms (cf. Figure 3).

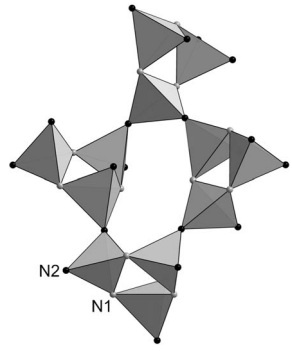

Figure 3. Building unit of the Si/N substructure of $Li_2CaSi_2N_4$. The [SiN_4] tetrahedrons form *dreier* rings, four of them build up *siebener* rings. N1 gray and N2 black.

The Si–N network builds up four channels per unit cell along [100], in which the cations are localized. The framework density (number of tetrahedral centers in a volume of 1000 Å^3) of $Li_2SrSi_2N_4$ is 19.5. Taking into account that [SiN_4] tetrahedra are roughly 20% larger than [SiO_4] tetrahedra, the framework of $Li_2MSi_2N_4$ does not meet the requirements for a zeolite-like structure. The coordination spheres of the two crystallographically independent Ca^{2+} sites are depicted in Figure 4.

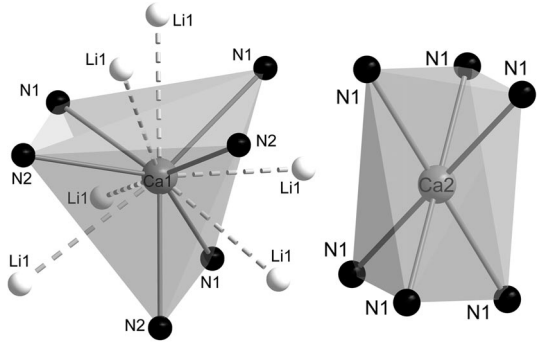

Figure 4. Coordination spheres of the two Ca^{2+} sites in $Li_2CaSi_2N_4$.

Regarding the Ca coordination, we observed a highly symmetrical surrounding of both Ca sites by six nitrogen atoms, forming a trigonal prism around the Ca1 site and a trigonal antiprism around the Ca2 site. The Ca–N distances (cf. Table 2) correspond well with other known lithium calcium nitridosilicates such as $Li_4Ca_3Si_2N_6$ [240.7(2)–281.9(2) pm] or $LiCa_3Si_2N_5$ [234.4(5)–284.3(5) pm].[18] The second coordination sphere of Ca1 [284.4(5)–289.3(5) pm] is built up from Li atoms, forming an additional trigonal prism.

Because of the larger ionic radius of Sr^{2+} compared to Ca^{2+} the Sr2 site is slightly differently coordinated for the $Li_2SrSi_2N_4$ compound. Here, the Sr2 site is coordinated by 6 N1 atoms and 6 N2 atoms. It can best be described as a 6+6 coordination of nitrogen, forming a distorted icosahedron (see Supporting Information, Figure S2). The Sr1 site is surrounded by six nitrogen atoms, similarly to the Ca1 site. The assignment of the coordination spheres of the metals was achieved by lattice energy calculation (MAPLE Madelung part of lattice energy, see Table 3 and section below).[29,30]

The Li-site in $Li_2CaSi_2N_4$ is coordinated by nitrogen in form of a distorted quadratic pyramid, whereas in $Li_2SrSi_2N_4$ the coordination of Li can be described in terms of a distorted tetrahedral surrounding. However, the LiN_n polyhedra in both compounds are connected via edges, re-

sulting in long Li···Li distances [$Li_2CaSi_2N_4$: 344.7(9) pm; $Li_2SrSi_2N_4$: 339(1) pm], rendering lithium ion conduction unlikely.

Lattice Energy Calculations (MAPLE)

Since both compounds exhibit slightly different coordination spheres, we performed additional lattice energy calculations with the program MAPLE to ensure electrostatic correctness. As mentioned the Ca2 and Sr2 sites exhibit different surrounding by nitrogen atoms due to their different ionic radii. Nevertheless, lattice energy calculations supported a sixfold coordination for Ca2 and 6+6 coordination for Sr2. The sum of the partial MAPLE values is in good agreement with the sum of constituting nitrides (cf. Table 3). Furthermore, the partial MAPLE values of the ions are in the normal range compared to other lithium nitridosilicates.[18]

Table 3. Results of MAPLE calculations [kJ/mol] for $Li_2MSi_2N_4$ (M = Ca, Sr; Δ = difference).

	Ca	Sr
$M(1)^{2+}$ (8*c*)[a]	1980	1748
$M(2)^{2+}$ (4*b*)	1747	1649
Si^{4+} (24*d*)	9789	9821
$N(1)^{3-}$ (24*d*)	5490	5447
$N(2)^{3-}$ (24*d*)	5526	5452
Li^{+} (24*d*)	670	712
Total MAPLE	44834	44580
Δ	1.2%	1.1%
Total MAPLE (2 Li_2SiN_2 + 1/3 Ca_3N_2 – 2/3 Li_3N): 43826 kJ/mol		
Total MAPLE (Li_2SiN_2 + $SrSiN_2$): 44094 kJ/mol		

[a] Typical partial MAPLE values [kJ/mol]: Ca^{2+}: 1800–2200; Sr^{2+}: 1500–2100; Si^{4+}: 9000–10200; $N^{[2]3-}$: 4600–6000; Li^{+}: 600–860.[31,32]

Solid-State MAS NMR

During the last years, a series of nitridosilicates have been characterized using solid-state MAS NMR spectroscopy, resulting in a δ scale for ^{29}Si from –28 ppm observed for reduced nitridosilicates ($SrSi_6N_8$)[33] to oxo-nitridosilicates (–68 ppm, $Ba_3Si_6O_9N_4$)[34] on the other end. The chemical shift of ^{29}Si in the case of [SiN_4] tetrahedrons are usually found in the region between –40 to –60 ppm. We performed solid-state MAS NMR spectroscopy on $Li_2SrSi_2N_4$ due to the availability of bulk material (HF furnace approach), the ^{29}Si MAS spectrum is depicted in Figure 5. It consists of an unresolved signal in the range of –55.7 ppm. The ^{7}Li solid-state NMR spectrum of $Li_2SrSi_2N_4$ (Figure 5) consists of an intense and broad isotropic peak centred at 2.0 ppm. The observed chemical shift value of 2.0 ppm is comparable to that of Li_2SiN_2 (δ = 1.7 ppm)[35] or $LiSi_2N_3$ (δ = 1.3 ppm).[36]

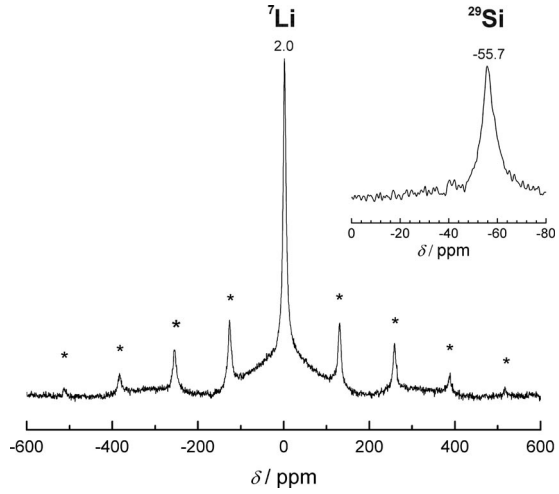

Figure 5. Solid-state MAS NMR spectra (^{7}Li and ^{29}Si, inset) of $Li_2SrSi_2N_4$. Rotation bands are indicated by asterisk (rotation frequency 25 kHz).

Electron Energy-Loss Spectroscopy (EELS)

To further confirm Li incorporation in the structure, we performed additional EELS measurements. To check for local variations, we conducted these measurements in a TEM. EELS is superior for light element detection compared to EDX which is not able to detect elements with atomic numbers <5. The Li-K edge (Figure 6) occurs at around 56 eV and shows a main peak at 64 eV and a smaller peak at ca. 57.5 eV. From this electron energy near edge structure (ELNES) information on the bonding can be extracted.[37] The Li-K ELNES is different compared to published data for example Li, $LiMn_2O_4$, and Li_2O which is related to the different bonding types.[38] However, a detailed analysis requires ab initio calculations which are beyond the scope of this contribution. Nevertheless, the EELS measurements clearly show that Li is incorporated in the structure. Furthermore, EELS confirmed the EDX chemical analysis and showed the presences of Si and N. The first peak of the Si-$L_{2,3}$ edge lies at around 106 eV and is visible in Figure 6, while the N-K edge occurs around 401 eV (see Supporting

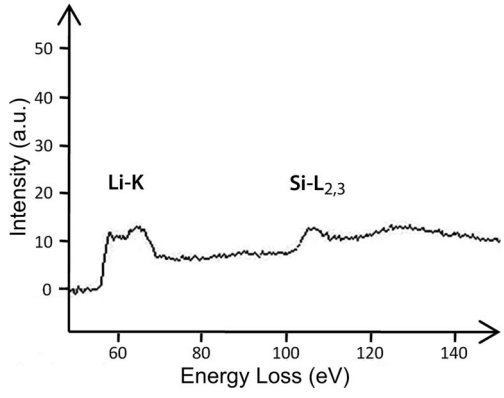

Figure 6. EELS spectrum of $Li_2SrSi_2N_4$. The energy loss region of the Li-K edge and Si-$L_{2,3}$ is shown. The background in front of the Li-K edge is subtracted.

Information; Figure S3). The Sr-$L_{2,3}$ lies at high energy losses of > 2080 eV and was not measured in the present work. High resolution TEM images (HRTEM) of $Li_2SrSi_2N_4$ confirmed the ordered structure (Figure 7).

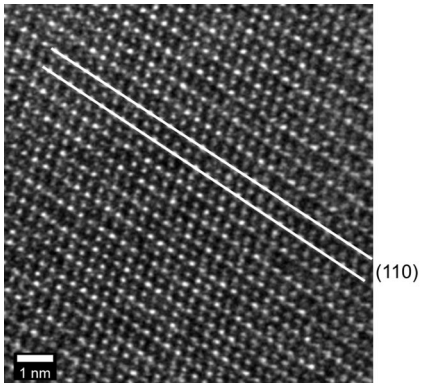

Figure 7. HRTEM image of $Li_2SrSi_2N_4$. The image was taken in <113> zone axis orientation.

Conclusions

With $Li_2MSi_2N_4$ (M = Ca, Sr) we present the first three-dimensional oxygen free lithium alkaline earth nitridosilicates. Two approaches led to these moisture and oxygen stable compounds, one comprising closed tantalum ampoules and the other using the open system of tungsten crucibles in a high-frequency furnace. The current investigation reveals that the amount of nitrogen during the synthesis allows for control of the dimensionality of the obtained lithium nitridosilicates. Accordingly, higher nitrogen amount gives access to highly condensed networks, even though the synthesis temperature is held constant. Hence, we are confident to gain more control over this relatively novel compound class. Particularly, investigations of these compounds with solid-state MAS NMR spectroscopic data of ^{7}Li and ^{29}Si as well as EELS measurements gave a deeper insight into this class of nitridosilicates.

Experimental Section

Synthesis: All manipulations were performed with rigorous exclusion of oxygen and moisture in flame-dried Schlenk-type glassware on a Schlenk line interfaced to a vacuum (10^{-3} mbar) line or in an argon-filled glove box (Unilab, MBraun, Garching, $O_2 < 0.1$ ppm, $H_2O < 0.1$ ppm). Argon (Messer-Griessheim, 5.0) was purified by passage through columns of silica gel (Merck), molecular sieves (Fluka, 4 Å), KOH (Merck, ≥ 85%), P_4O_{10} (Roth, ≥ 99%, granulate) and titanium sponge (Johnson Matthey, 99.5%, grain size ≤ 0.8 cm) at 700 °C.

The procedure for reactions in supercritical NH_3 is described in the following: The starting material (strontium, Sigma–Aldrich, 99.99%, pieces) was introduced into a Parr high-pressure vessel (Type 4740) with a Parr gage block (Type 4316) and connected to a vacuum/inert gas line. A sufficient amount of ammonia was condensed by cooling the vessel to –80 °C. The reaction vessel was closed and slowly warmed up to room temperature and then heated at 10 °C/min to the final reaction temperature. A pressure of 4500 psi (ca. 310 bar) was observed during the reaction. After 5 d the vessel was cooled down to room temperature and the pressure was reduced carefully by opening the valve of the unit. Finally, the vessel was opened in an argon-filled glove box. A finely crystalline product [e.g. $Sr(NH_2)_2$] was isolated and analyzed by IR spectroscopy and powder XRD (Stoe STADI P diffractometer; transmission mode, Mo-$K_{\alpha1}$ radiation, λ = 71.073 pm).

Lithium and Li_3N were purchased from Alfa Aesar (99.9% and 99.4%, respectively) and $Si(NH)_2$ was synthesized according to the literature.[39]

For the synthesis of $Li_2MSi_2N_4$ (M = Ca, Sr) tantalum tubes (wall thickness 0.5 mm, internal diameter 10 mm, length 300 mm) were cleaned in a mixture of aqueous HNO_3 (concd.) and HF (40%). They were weld-shut under a pressure of 1 bar purified Argon in an arc furnace. The crucible holder was water cooled in order to avoid the start of the reaction during welding.

Single crystals of $Li_2MSi_2N_4$ (M = Ca, Sr) were synthesized from 20 mg Li (2.87 mmol), 67 mg $Si(NH)_2$ (1.15 mmol), 28 mg LiN_3 (0.57 mmol) and 23 mg Ca (0.57 mmol) or 50 mg Sr (0.57 mmol, respectively) in closed tantalum crucibles placed in silica tubes. The silica tube (under argon) was placed in the middle of a tube furnace. The temperature was raised to 900 °C (rate 120 °C h^{-1}), maintained for 24 h, subsequently cooled to 500 °C (rate 5 °C h^{-1}) and finally quenched to room temperature by switching off the furnace.

For bulk samples of $Li_2SrSi_2N_4$ for solid-state MAS NMR and EELS measurements 50 mg $Si(NH)_2$ (0.86 mmol), 50 mg Li_3N (1.44 mmol) and 51.5 mg $Sr(NH_2)_2$ (0.43 mmol) were placed in a tungsten crucible under an argon atmosphere inside a glove box. After placing the crucible into the water cooled quartz reactor of a radio-frequency furnace (type IG 10/200 Hy, frequency: 200 kHz, max. electrical output: 12 kW, Hüttinger, Freiburg)[19] under a N_2 atmosphere, the temperature was raised to 900 °C within 12 h. After 12 h the temperature was cooled to 700 °C within 24 h and further cooled to 400 °C within 24 h. subsequent quenching to room temperature in 30 min yielded colorless $Li_2SrSi_2N_4$. The identity and purity of the product was verified by X-ray powder diffraction. The X-ray powder patterns have also been double-checked by comparison with theoretical diffraction patterns calculated from single-crystal X-ray diffraction data (see Supporting Information).

Scanning Electron Microscopy (SEM) and Energy Dispersive X-ray Spectroscopy (EDX): Scanning electron microscopy was performed on a JEOL JSM-6500F equipped with a field emission gun at an acceleration voltage of 10 kV. Samples were prepared by placing single crystals on adhesive conductive pads and subsequently coating them with a thin conductive carbon film. Each EDX spectrum (Oxford Instruments) was recorded with the analyzed area limited on one single crystal to avoid the influence of possible contaminating phases. Analysis of three spots per crystallite showed average atomic M/Si/O/N compositions (%) of M = Sr: 33.6(2):28.0(2):0:33.8(4) and M = Ca: 21.1(2):33.2(2):3.0(2):42.6(4). These results confirm the presence of the elements (lithium cannot be detected) and are in agreement with the compositions obtained from single-crystal X-ray studies (the calculated values M/Si/O/N are M = Sr: 41.0:26.3:0:26.22 and M = Ca: 24.2:33.8:0:33.7). Lithium cannot be observed by EDX methods.

X-ray Diffraction: By inspection under a microscope integrated in a glove box, colorless single crystals of the title compound were isolated from residual lithium and enclosed in glass capillaries. Single-crystal X-ray diffraction data were collected on a STOE IPDS diffractometer (Mo-K_α radiation; see Table 4). The program package SHELX97 was used for structure solution and refinement.[40]

Table 4. Crystallographic data of $Li_2MSi_2N_4$ (M = Ca, Sr).

Formula	$Li_2CaSi_2N_4$	$Li_2SrSi_2N_4$
Formula mass [g mol^{-1}]	166.16	213.70
Crystal system	cubic	cubic
Space group	$Pa\bar{3}$ (no. 205)	$Pa\bar{3}$ (no. 205)
Cell parameters [pm]	a = 1056.9(12)	a = 1071.37(12)
Cell volume [10^6 pm^3]	V = 1180.7(2)	V = 1229.8(2)
Formula units/cell	12	12
Crystal size [mm^3]	0.1 × 0.08 × 0.07	0.3 × 0.28 × 0.26
$\rho_{calcd.}$ [g·cm^{-3}]	2.805	3.463
M [mm^{-1}]	2.026	13.567
F(000)	984	1200
Diffractometer	Stoe IPDS 1	Stoe IPDS 1
Temperature [K]	295(2)	293(2)
Radiation, monochr.	Mo-K_α (λ = 71.073 pm), graphite	Mo-K_α (λ = 71.073 pm), graphite
Absorption correction	multi scan	numerical
θ range [°]	3.34–28.7	3.29–29.98
Measured reflections	6662	7811
Independent reflections	513	602
Observed reflections	412	528
Refined parameters	42	42
GoF	0.979	1.118
R indices [$F_o^2 \geq 2\sigma$ (F_o^2)]	R_1 = 0.0331, $wR2$ = 0.0795	R_1 = 0.0427, $wR2$ = 0.1187
R indices (all data)	R_1 = 0.0439, $wR2$ = 0.0839[a]	R_1 = 0.0476, $wR2$ = 0.1227[b]
Max./min. residual electron density/e Å^{-3}	0.388/–0.434	3.042/–1.677

[a] $w = 1/[\sigma^2(F_o^2) + (0.0584\ P)^2 + 0.00\ P]^{-1}$ where $P = (F_o^2 + 2\ F_c^2)/3$. [b] $w = 1/[\sigma^2(F_o^2) + (0.0893\ P)^2 + 0.00\ P]^{-1}$ where $P = (F_o^2 + 2\ F_c^2)/3$.

CSD-421548 (for $Li_2CaSi_2N_4$) and -421549 (for $Li_2SrSi_2N_4$) contain the supplementary crystallographic data for this paper. These data can be obtained free of charge from the Fachinformationszentrum Karlsruhe, 76344 Eggenstein-Leopoldshafen, Germany (Fax: +49-7247-808-666; E-mail: crysdata@fiz-karlsruhe.de), on quoting the depository number.

Powder diffraction data were collected in Debye–Scherrer geometry on a STOE Stadi P powder diffractometer with Ge(111)-monochromatized Cu-$K_{\alpha1}$ radiation (λ = 1.5406 Å).

Solid-State MAS NMR: Experiments were performed at 11.74 T on a Bruker DSX 500 Advance FT spectrometer equipped with a commercial 2.5 mm triple-resonance MAS probe at the ^{29}Si and ^{7}Li frequencies of 99.385 MHz and 194.399 MHz, respectively. All experiments were performed in ZrO_2 rotors at room temperature. The chemical shifts of ^{29}Si and ^{7}Li are reported using the frequency ratios published by IUPAC [δ scale relative to 1% tetramethylsilane (TMS) in $CDCl_3$].[41] The ^{29}Si MAS-NMR spectrum was acquired with a 90° pulse length of 3.0 µs, a recycle delay of 64000 s and at a sample spinning frequency of 25 kHz. The ^{7}Li MAS-NMR spectrum was acquired with a 90° pulse length of 2.5 µs, a recycle delay of 64 s and at a sample spinning frequency of 25 kHz.

Electron Energy-Loss Spectroscopy (EELS): EELS measurements were conducted in a TEM using a FEI Titan 80–300 keV. This electron microscope is equipped with an energy-dispersive X-ray detector from EDAX and a post-column energy filter (GIF Tridiem from Gatan) for analytical investigations. The EELS data were acquired in diffraction mode averaging over an area of about 150 nm to prevent beam damage. A 2 mm entrance aperture of the spectrometer was used resulting in a collector angle of 13.5 mrad.

EELS data were acquired with an energy resolution of about 0.8–1 eV as determined by the full width of half maximum of the zero loss peak. Data were taken with a dispersion of 0.2 eV/channel leading to acquisition times ranging between 10s for the Li-K and Si-$L_{2,3}$ edges, and 50 s for the spectra containing the N-K edge (not shown). All data were corrected for dark current and detector channel to channel gain variation. The pre-edge background of the Li-K was extrapolated using a 1st order-log-polynomial function and subtracted from the original data. For the other edges the standard power law function can be used.[37] A plural scattering deconvolution was not required due to the low thickness of the investigated areas.

Supporting Information (see also the footnote on the first page of this article): PXRD pattern of $Li_2SrSi_2N_4$ in comparison to the simulation from single-crystal structure analysis and final atomic coordinates, and equivalent displacement parameters of $Li_2SrSi_2N_4$.

Acknowledgments

We are indebted to the following people for conducting the physical measurements: Dr. Jörn Schmedt auf der Günne and Christian Minke (solid-state NMR), Dr. Oliver Oeckler and Thomas Miller (single-crystal X-ray diffractometry), [all Department of Chemie, University of München (LMU)]. Sandra Kiese and Christian Ziegler are kindly acknowledged for assistance of TEM and EELS data analysis. The authors gratefully acknowledge financial support from the Fonds der Chemischen Industrie (FCI) and the Deutsche Forschungsgemeinschaft (DFG) (DFG, project SCHN 377/14-1).

[1] W. Schnick, *Int. J. Inorg. Mater.* **2001**, *3*, 1267–1272.
[2] Y. Q. Li, G. deWith, H. T. Hintzen, *J. Solid State Chem.* **2008**, *181*, 515–524.
[3] R. Mueller-Mach, G. Mueller, M. R. Krames, H. A. Höppe, F. Stadler, W. Schnick, T. Juestel, P. Schmidt, *Phys. Status Solidi A* **2005**, *202*, 1727–1732.
[4] X. Piao, T. Horikawa, H. Hanzawa, K. Machida, *Appl. Phys. Lett.* **2006**, *88*, 161908/1–161908/3.
[5] R.-J. Xie, N. Hirosaki, *Sci. Technol. Adv. Mater.* **2007**, *8*, 588–600.

[6] R.-J. Xie, N. Hirosaki, N. Kimura, K. Sakuma, M. Mitomo, *Appl. Phys. Lett.* **2007**, *90*, 191101/1–191101/3.
[7] W. Schnick, H. Huppertz, *Chem. Eur. J.* **1997**, *3*, 679–683.
[8] H. Huppertz, W. Schnick, *Angew. Chem.* **1996**, *108*, 2115–2116; *Angew. Chem. Int. Ed. Engl.* **1996**, *35*, 1983–1984.
[9] H. Huppertz, W. Schnick, *Z. Anorg. Allg. Chem.* **1997**, *623*, 212–217.
[10] H. Huppertz, W. Schnick, *Acta Crystallogr., Sect. C: Cryst. Struct. Commun.* **1997**, *53*, 1751–1753.
[11] T. Schlieper, W. Milius, W. Schnick, *Z. Anorg. Allg. Chem.* **1995**, *621*, 1380–1384.
[12] M. Zeuner, F. Hintze, W. Schnick, *Chem. Mater.* **2009**, *21*, 336–342.
[13] M. Zeuner, P. J. Schmidt, W. Schnick, *Chem. Mater.* **2009**, *21*, 2467–2473.
[14] H. Yamane, F. J. DiSalvo, *J. Alloys Compd.* **1996**, *240*, 33–36.
[15] Z. A. Gál, P. M. Mallinson, H. J. Orchard, S. J. Clarke, *Inorg. Chem.* **2004**, *43*, 3998–4006.
[16] M. Zeuner, S. Pagano, P. Matthes, D. Bichler, D. Johrendt, T. Harmening, R. Pöttgen, W. Schnick, *J. Am. Chem. Soc.* **2009**, *131*, 11242–11248.
[17] S. Lupart, M. Zeuner, S. Pagano, W. Schnick, *Eur. J. Inorg. Chem.* **2010**, 2636–2641.
[18] S. Pagano, S. Lupart, M. Zeuner, W. Schnick, *Angew. Chem.* **2009**, *121*, 6453; *Angew. Chem. Int. Ed.* **2009**, *48*, 6335.
[19] W. Schnick, H. Huppertz, R. Lauterbach, *J. Mater. Chem.* **1999**, *9*, 289–296.
[20] T. Schlieper, W. Schnick, *Z. Anorg. Allg. Chem.* **1995**, *621*, 1037–1041.
[21] P. Eckerlin, A. Rabenau, H. Nortmann, *Z. Anorg. Allg. Chem.* **1967**, *353*, 113–121.
[22] T. Endo, Y. Sato, H. Takizawa, M. Shimada, *J. Mater. Sci. Lett.* **1992**, *11*, 424–426.
[23] M. Wintenberger, R. Marchand, M. Maunaye, *Solid State Commun.* **1977**, *21*, 733–735.
[24] Liebau established the terms *zweier*, *dreier*, *vierer*, *fünfer* chains. Thereby, a *zweier* chain can be described as *two* polyhedra within one repeating unit of the linear part of the chain. The terms derive from the German numerals *drei* (3), *vier* (4), *fünf* (5) etc. by adding the suffixing "er" to the numeral (F. Liebau, *Structural Chemistry of Silicates*, Springer, Berlin, **1985**).
[25] M. O'Keeffe, *Acta Crystallogr., Sect. A: Found. Crystallogr.* **1992**, *48*, 670–673.
[26] M. Marezio, J. P. Remeika, P. D. Dernier, *Acta Crystallogr., Sect. B: Struct. Sci.* **1969**, *25*, 965–970.
[27] N. L. Ross, R. J. Angel, *J. Solid State Chem.* **1991**, *90*, 27–30.
[28] B. Eisenmann, M. Jakowski, H. Schaefer, *Mater. Res. Bull.* **1982**, *17*, 1169–1175.
[29] R. Hübbenthal, *Programm zur Berechnung des Madelunganteils der Gitterenergie*, rel. 4, University of Gießen, **1993**.
[30] R. D. Shannon, *Acta Crystallogr., Sect. A: Cryst. Found. Crystallogr.* **1976**, *32*, 751–767.
[31] H. A. Höppe, *Doctoral* Thesis, University of Munich, **2003**.
[32] K. Köllisch, *Doctoral* Thesis, University of Munich, **2001**.
[33] F. Stadler, O. Oeckler, J. Senker, H. A. Höppe, P. Kroll, W. Schnick, *Angew. Chem.* **2005**, *117*, 573–576; *Angew. Chem. Int. Ed.* **2005**, *44*, 567–570.
[34] F. Stadler, W. Schnick, *Z. Anorg. Allg. Chem.* **2006**, *632*, 949–954.
[35] S. Pagano, M. Zeuner, S. Hug, W. Schnick, *Eur. J. Inorg. Chem.* **2009**, 1579–1584.
[36] P. Kempgens, R. K. Robin, D. P. Thompson, *Solid State Nucl. Magn. Reson.* **1999**, *15*, 109–118.
[37] R. F. Egerton, *Electron Energy-Loss Spectroscopy in the Electron Microscope*, 2. edition, New York: Plenum Press **1996**.
[38] V. Mauchamp, F. Boucher, G. Ouvrard, P. Moreau, *Phys. Rev. B: Condens. Matter* **2006**, *74*, 115106/1-115106/10.
[39] H. Lange, G. Wötting, G. Winter, *Angew. Chem.* **1991**, *103*, 1606–1625; *Angew. Chem. Int. Ed. Engl.* **1991**, *30*, 1579–1597.
[40] G. M. Sheldrick, *Acta Crystallogr., Sect. A: Cryst. Found. Crystallogr.* **2008**, *64*, 112–122.
[41] R. K. Harris, E. D. Becker, S. M. Cabral de Menezes, R. Goodfellow, P. Granger, *Solid State Nucl. Magn. Reson.* **2002**, *22*, 458–483.

Received: June 21, 2010
Published Online: September 13, 2010

